

Guided port injection of hydrogen as an approach for reducing cylinder-to-cylinder deviations in spark-ignited H₂ engines – a numerical investigation

Jung, P. E., Walter, N. and Guenther, M.
RPTU University of Kaiserslautern-Landau

Abstract

The reduction of anthropogenic greenhouse gas emissions and ever stricter regulations on pollutant emissions in the transport sector require research and development of new, climate-friendly propulsion concepts. The use of renewable hydrogen as a fuel for internal combustion engines promises to provide a good solution especially for commercial vehicles. For optimum efficiency of the combustion process, hydrogen-specific engine components are required, which need to be tested on the test bench and analysed in simulation studies. This paper deals with the simulation-based investigation and optimisation of fuel injection in a 6-cylinder PFI commercial vehicle engine, which has been modified for hydrogen operation starting from a natural gas engine concept. The focus of the study is on a CNG-derived manifold design which has been adapted with regard to the injector interface and is already equipped with so-called gas injection guiding tubes for targeted fuel injection in front of the intake runners of the individual cylinders. Significant deviations between the averaged cylinder pressure profiles of the individual cylinders observed on the test bench point to an issue with the equal distribution of the fuel supply to the individual cylinders. A subsequent 3D CFD simulation of the internal manifold flow showed geometry-induced turbulence of the fresh air flow in the area of the hydrogen supply outlet of several cylinders, which can lead to variations in cylinder-specific fuel quantities. In order to minimise the influence of the air flow in the manifold on the fuel injection, a dedicated injection guide concept for the gas injection tubes in the intake manifold has been designed with the aim of moving the position of hydrogen injection closer to the intake valves. In this study, this concept is analyzed based on first results obtained from a detailed 3D CFD simulation, especially in terms of the uniformity of hydrogen distribution between the cylinders, mixture formation and the effect on combustion.

Introduction

The transport sector accounts for around a third of global final energy consumption and has the highest annual growth rates of around 3 to 4 %. This is reflected in the fact that around 62 % of the oil converted into drive energy worldwide is attributable to the transport of people or goods [1]. Reducing CO₂ emissions in the transport sector is therefore one of the core disciplines in the development of modern drive concepts today. While the trend in the passenger transport sector in finding solutions for the climate-friendly transport of people and goods is increasingly moving towards battery-electric vehicles and vehicles based on fuel cell technology [2], these drive forms are only suitable to a limited extent for commercial vehicle drives or mobile machinery due to a different requirement profile. In the range of low

specific loads (i.e. the typical power range of passenger cars), combustion engines are inferior to the efficiency of a fuel cell system, but this situation changes at high specific loads, which are frequently required in real operation of commercial vehicles. In this power range, the efficiency of an internal combustion engine may even exceed the efficiency of a fuel cell, cf. Figure 1.

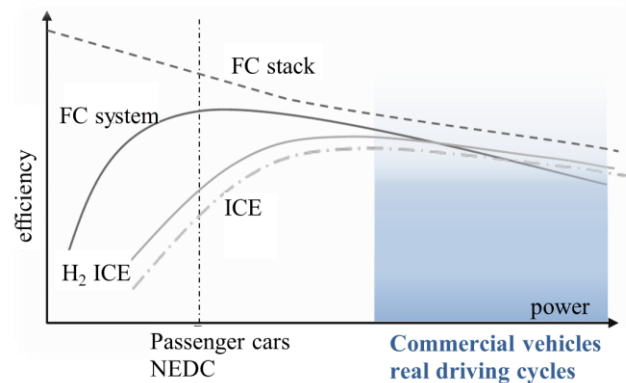


Figure 1. Qualitative comparison of the load-dependent efficiency curves of different types of propulsion systems [3]

To provide CO₂-neutral drive power, conventional combustion engines can be converted for operation with alternative fuels derived from regenerative sources. PFI (port fuel injection) solutions are an attractive option in this context due to their comparatively low conversion costs and low required fuel supply pressures. As an alternative fuel for spark-ignition combustion processes, hydrogen is one of the options which are frequently discussed in this context. Provided that renewable electricity is used for hydrogen production e.g. by electrolysis (so-called green hydrogen [4]), this is not only a CO₂-neutral, but a completely CO₂-free fuel. The direct use of hydrogen eliminates the subsequent processing steps necessary for conversion into other synthetic fuels (e.g. methanisation or Fischer-Tropsch synthesis), which has an additional positive effect on the overall efficiency of the process. Since water as the starting material required for production is available in virtually infinite quantities, there is also no competition with food production as it might be the case with some types of biofuels.

Due to its wide ignition limits [5], hydrogen is particularly suitable for use in ultra-lean combustion processes. This means that efficiency values similar to those of a diesel engine can be achieved. Due to the comparatively "cold combustion" in lean-burn operation, nitrogen oxide emissions also remain at a low level over a wide range of the engine map [6]. However, due to the low density of hydrogen, PFI engine concepts can also suffer from charging losses during gas exchange, which can lead to a drop both in performance and in efficiency. If due to unfavorable flow conditions in the intake manifold hydrogen is deflected too much during injection, an ignitable mixture might be formed in the intake manifold under certain circumstances, leading to an increased risk of spontaneous unwanted reaction (so-called backfire) due to the low ignition energy of hydrogen. This reduces the engine's potential for reaching high specific power [7]. For these reasons, the supply of hydrogen into the manifold should be as close to the intake valves as possible in order to precisely control the supply to the individual cylinders and avoid cross-influences caused by turbulence of the aspirated air flow.

The study presented here analyses the fuel supply of a hydrogen-powered six-cylinder commercial vehicle engine derived from a Daimler Truck M936G engine and converted to hydrogen operation as part of a research project. The fuel supply is based on a multi-point PFI concept, with hydrogen injected into the manifold in the area of the intake runners through separate injectors for the individual cylinders. Investigations on the test bench revealed issues in the equal distribution of hydrogen to the different cylinders, resulting in strongly varying IMEP between the cylinders. In order to understand the underlying phenomena better, the system was analysed through 3D CFD simulation. The variations observed in the individual cylinder pressure curves could be traced back to design-related root causes affecting both the air supply and the fuel injection. As an approach to solve this issue, a modified injection guiding concept was designed aiming at an optimisation of the fuel supply to the individual cylinders. In addition, the new design of the injection guiding tubes should also reduce the proportion of residual hydrogen remaining in the manifold in order to minimise the risk of backfire. After a brief overview of the experimental and simulation set-up, the first results of this study are presented, followed by an in-depth analysis and comparison of the optimised design with the basic injection tube.

Experimental Setup

All experimental tests were carried out on a DT M936G engine modified for operation with hydrogen. The test cell is supplied with fuel from a 300 bar bundle system providing hydrogen of purity class 3.0 (hydrogen content $\geq 99.9\%$ by volume, specifications cf. Table 1). The fuel is supplied to the engine via a hydrogen-specific gas pressure regulator (inlet pressure 25 bar), which in turn is connected to the hydrogen supply system of the test bench. From the gas pressure regulator, the fuel is fed into a common rail, which is kept at a pressure of 4 to 14 bar (relative) by the gas pressure regulator. From the fuel rail, the hydrogen is fed to the injectors via steel flex lines. Six side-fed injectors supplied by Hoerbiger are used for port injection. The mixture is ignited through series Bosch CNG spark plugs. The valve train was taken over from the base engine and does not provide any variability with regard to cam phasing. The technical specifications of the engine can be found in Table 2.

The load was applied to the test engine through a Horiba HD 380 asynchronous motor controlled via a Horiba Stars test bench automation system. The cylinder pressures of all six cylinders were recorded with Kistler 6045 piezo-electric pressure sensors, while the inlet and outlet pressure were recorded with Kistler 4011 and Kistler

4049 piezo-resistive pressure sensors. All pressure signals were collected through an AVL X-Ion system with AVL Indicom used for evaluation and visualisation. Besides, the engine was equipped with several low-frequency pressure measuring points using Endress+Hauser Cerabar PMP21 sensors, and several temperature measuring points using either PT 100 resistance thermometers or thermocouples type N, both provided by Omega Engineering. A Bronkhorst MFM F-116BI Coriolis sensor was used to measure the fuel mass flow. The air-fuel ratio was determined using a Bosch LSU 5.1 broadband lambda probe in combination with an ETAS ES 635.1 lambda meter. The operating parameters, apart from the accelerator pedal position and engine speed, were set using a modified H₂-specific control unit. The numerical analysis was carried out using the 3D CFD simulation software AVL Fire.

Table 1. Hydrogen specifications for the investigation

| | |
|-------------------------------|---|
| Purity classification | H ₂ 3.0, H ₂ content ≥ 99.9 Vol.-% |
| Lower heating value | 33,33 kWh/kg |
| Density | 0.0899 kg/Nm ³ |
| Stoichiometric air-fuel ratio | 34.3 (-) |

Table 2. Technical data of the test engine

| | |
|-------------------------------|------------------------|
| Displacement | 7698 cc |
| Stroke | 135 mm |
| Bore | 110 mm |
| Connecting Rod | 215 mm |
| Compression ratio | 11.8:1 |
| Number of Valves per Cylinder | 4 |
| Inlet Valve Open | 14° ATDC @ 0.2 mm lift |

Methodology

For a more precise analysis of the deviations between the pressure curves of the individual cylinders observed during test bench operation, a reference measurement was carried out at 1200 rpm and an average IMEP of 6 bar, without EGR and keeping MFB₅₀ constant at 8° CA after firing TDC. This revealed significant deviations between the indicated mean pressures of the individual cylinders of up to 1 bar (see Figure 2). The resulting coefficient of variation of IMEP was 4.1 %. The largest deviation was found between cylinder 1 (max. IMEP) and cylinder 3 (min. IMEP).

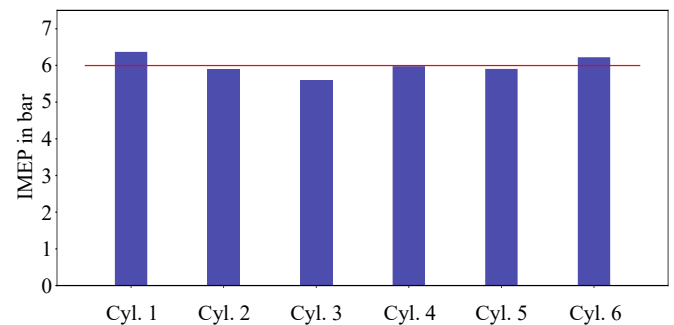


Figure 2. Reference measurement results of IMEP (cylinders 1 to 6) to analyse the deviations of the individual cylinders

Based on this data and after analysing the geometric features of the intake manifold and particularly the region of mixture formation, the design of the H₂-specific intake manifold was identified as a possible cause of the aforementioned problem with regard to equal distribution of hydrogen to the engine cylinders. Due to the installation situation in the vehicle from which the base engine originates, the fresh air is fed into the manifold at the point in the red circle in Figure 3. The orange marking highlights a flow deflection plate taken over from the design of the base engine's original intake manifold. The deflection plate splits the manifold cross-section vertically at the position of cylinders 4 to 6 to prevent the charge air flow entering the manifold from interacting with the directly opposite intake ports of these three cylinders (the corresponding region is marked in yellow in Fig. 3). This was intended to have a positive effect on the equal distribution of the charge air flow (compared to the variant without flow deflection plate and therefore in interaction with the opposing intake runners). However, depending on which cylinder is currently aspirating, the air flow in the manifold is significantly deflected. The study discussed in the following analyses the intake flow into cylinders 1 and 3.

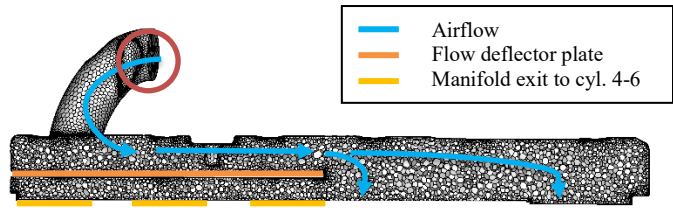


Figure 3. Qualitative illustration of the flow inside the intake manifold for the outlets to cylinders 1 and 3

To confirm this assumption and to analyse the effect of the geometric properties on the flow conditions inside the H₂-specific manifold and the resulting influence on fuel injection, a CFD simulation of the internal flow of the manifold was carried out first. Particular attention was paid to the flow characteristics in the area in front of the inlet ducts of cylinders 1 and 3. Based on this, a modified injection guiding tube was designed which – in contrast to the Y-shaped basic variant – injects hydrogen only into one of the two inlet ducts. The modified version is designed in such a way that it is possible to choose between injecting into the filling port or into the swirl port by rotating it around the fastening axis. For the current analysis, however, only the injection into the filling port of the engine will be considered. Figure 4 shows the basic Y-shaped version of the injection guide (in orange) in the original installation position. The installation position was selected so that the hydrogen is still injected into the manifold and not into the individual intake runners.

In order to simplify the comparison of the simulation results with those of the test bench investigations, the boundary conditions were selected based on operating points that had already been measured experimentally. The entering total air mass flow was deliberately selected when modelling the internal flow of the manifold in order to reproduce the flow around the deflection plate as accurately as possible. It was carried out under the assumption of a stationary flow, a total air mass flow of 400 kg/h and a pressure of 1.5 bar. Fuel injection and mixture preparation were simulated in a range from 370° to 540° crank angle. The boundary conditions and the initial conditions were chosen based on a selected operating point from the test bench (cf. Tables 3 and 4). A RANS approach with k-zeta-f turbulence model was used for modelling the characteristics of the turbulent flow.

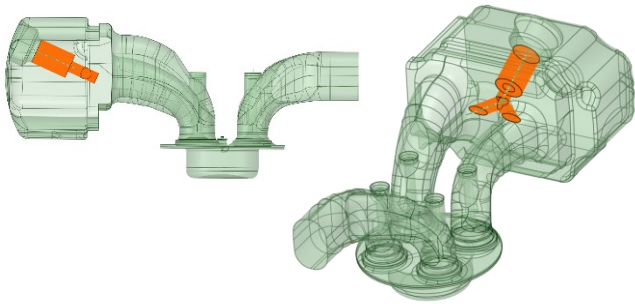


Figure 4. Surface model visualising the positioning of the basic injection tube variant

Table 3. Boundary conditions for the simulation of hydrogen injection

| | |
|---|------------------|
| Total air mass flow | 400 kg/h |
| Inlet pressure | 1.5 bar |
| Inlet temperature | 308 K |
| Wall temperature head, liner and cylinder | 510 K |
| Injected fuel mass | 33 mg |
| Fuel temperature | 293 K |
| Rail pressure | 9 bar |
| Start of injection | 20° CA after TDC |

Table 4. Initial conditions for the simulation of hydrogen injection

| | |
|---------------------------------------|-----------------------------------|
| Intake port turbulence kinetic energy | 5 m ² /s ² |
| Intake port pressure | 1.5 bar |
| Intake port temperature | 320 K |
| Cylinder turbulence kinetic energy | 8 m ² /s ² |
| Cylinder pressure | 0.98 bar (begin of intake stroke) |
| Cylinder temperature | 853 K |

During injection, the hydrogen was assumed to flow out of the cross section of the respective guiding tubes, with the direction of the injection jet being determined by their centre line. The influence of the fuel guiding tube design on the outflow behaviour, which has been neglected here, will be analysed in following studies.

Results and Discussion

The results of the numerical modelling of the stationary flow inside the manifold are shown in Figures 5 to 10, including the magnitude (colour gradient) and direction (vectors) of the flow velocity as well as the course of the streamlines in the relevant sectional view for each case. Figures 5 and 6 show a horizontal section through the manifold. It is obvious that the flow conditions at the position of the injector outlet openings (marked in red) are differing between the cylinders. In the area of cylinder 3 (Figure 5), the fresh air undergoes a significant deflection of the flow direction, which also means that part of the air flow is deflected in the direction of cylinders 1 and 2.

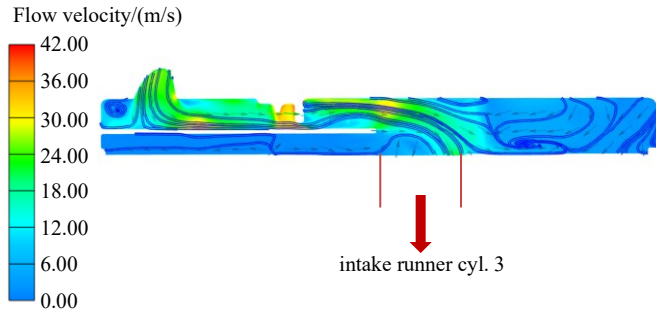


Figure 5. Horizontal sectional view of the manifold internal flow velocity (cylinder 3 aspirating)

From Figure 6 it is obvious that the flow of charge air (red area) is guided much better into the direction of cylinder 1 during its aspiration phase. This can be attributed to the lower rate of change of the direction of the flow entering the manifold. The vortex area near the exit to cylinder 3 again indicates the formation of a wake area in the region directly at the end of the flow deflection plate, which may also have a negative influence on the flow towards cylinders 4 to 6.

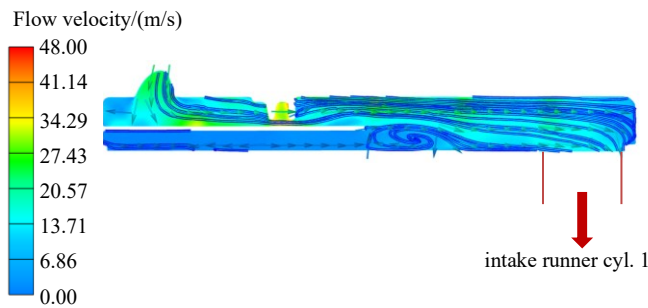


Figure 6. Horizontal sectional view of the manifold internal flow velocity (cylinder 1 aspirating)

Figures 7 and 8 each show a vertical section through the manifold. The sectional plane runs at the height of the outlet at the end of the injection guiding tube, assuming the Y-shaped basic variant shown above. Both at the exit of the manifold to the intake runner of cylinder 3 (Figure 7) and at the corresponding exit to cylinder 1 (Figure 8), a vortex area is created which has its centre approximately in the area of the outlet of the injection guiding tubes in the manifold. The flow around this intake could be the cause for the formation of this vortex area, but this has not been investigated in more detail yet. In effect, this can lead to the injection flow being partially deflected from its intended flow direction as originally determined during design and not being completely fed to the respective cylinder during gas exchange.

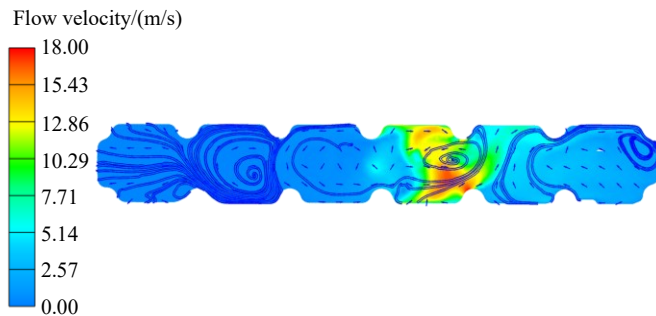


Figure 7. Vertical sectional view of the manifold internal flow velocity (cylinder 3 aspirating)

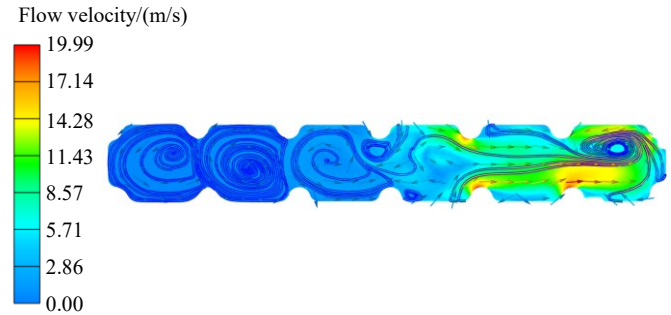


Figure 8. Vertical sectional view of the manifold internal flow velocity (cylinder 1 aspirating)

The longitudinal sections through the centre axis of the fuel injection guide shown in Figures 9 and 10 also indicate the formation of vortex regions in the area just in front of the intake ports, which can lead to an incomplete flow of hydrogen into the cylinder. When redesigning the guiding tubes, care should therefore be taken to ensure that the injected fuel can interact well with the supplied fresh air in terms of good mixture formation, but is also fed to the intended cylinder as unaffected as possible by the vortex areas in the manifold. For this reason, a positioning of the injection guiding tubes inside the intake ports was chosen.

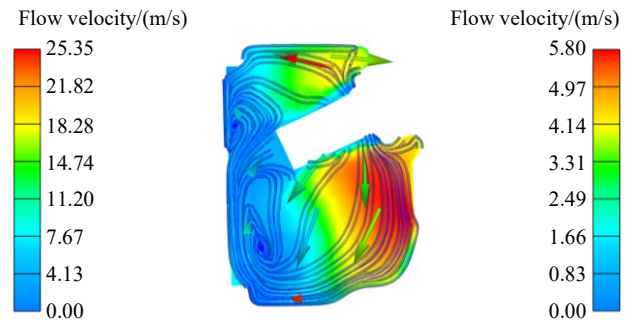


Figure 9. Longitudinal sectional view through the centre axis of the fuel injection guide of the manifold internal flow velocity (focus on cylinder 3)

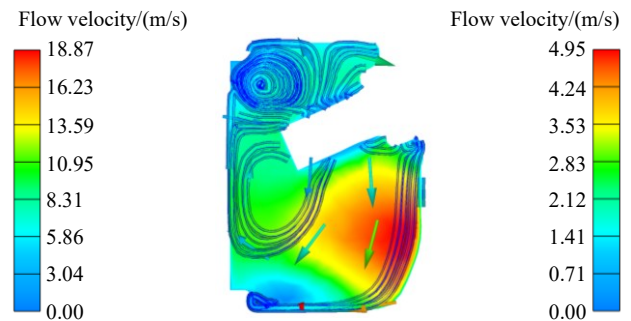


Figure 10. Longitudinal sectional view through the centre axis of the fuel injection guide of the manifold internal flow velocity (focus on cylinder 1)

The modified fuel injection tube developed based on the knowledge gained about the properties of the manifold internal flow is shown in orange in Figure 11. In order not to reduce the effective duct cross-section excessively, the injection tube was designed in such a way that, when installed, it protrudes only approx. 20 mm into the filling port of the engine. The rotational alignment was selected so that the imaginary extension of the fuel outlet direction is oriented towards the inlet valve.

For the simulation runs discussed in the following, injection only into the filling port of the engine was chosen.

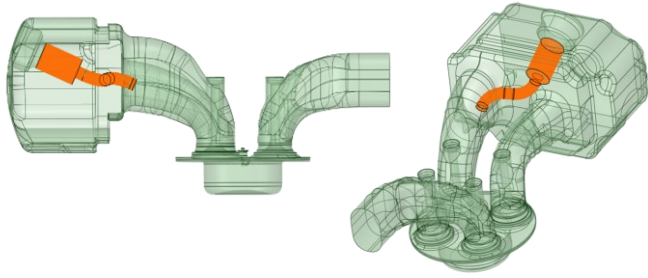


Figure 11. Surface model for visualising the positioning of the modified injection tube variant

In order to determine the effects of the modified fuel injection tubes on the fuel injection process, both variants were simulated in transient simulation runs assuming the boundary conditions listed above. Figure 12 shows the situation at the start of the injection process at 380.5° CA and at 395° CA for the modified variant.

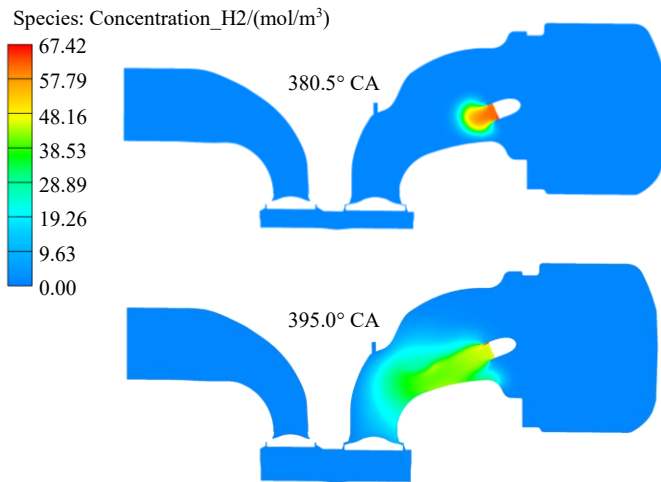


Figure 12. Visualisation of the hydrogen species concentration at 380.5° CA and at 395° CA (modified variant)

As the amount of fuel supplied to the cylinder directly influences the IMEP, the species concentration for hydrogen is used for analysis in the following discussion. It can be seen that shortly after the start of fuel injection at 400° CA, the first accumulations of hydrogen form in the intake manifold due to the non-optimal alignment of the Y-shaped base variant, see Figure 13. Although the majority of the injected fuel is fed to the intact port, the spray first hits the region below the intake runner (red circular marking), where part of the fuel spray is deflected and accumulates in the area in front of the intake ports. This is caused by the orientation of the injection tube, but is unavoidable due to the design of the manifold.

In contrast, it is obvious from Figure 14 that the fuel jet cannot be deflected at the outer area in front of the intake runner due to the protrusion of the modified fuel injection tube into the intake port. Therefore, only a marginal hydrogen accumulation forms in the area in front of the intake port, which could be caused by a backlog effect due to the intake valves opened to only approx. 1 mm at this time. This might be avoided by further optimization of the injection timing. As the entire fuel quantity is supplied through a single injection tube per

cylinder in the modified variant, a higher fuel concentration in the intake port can be observed as the result.

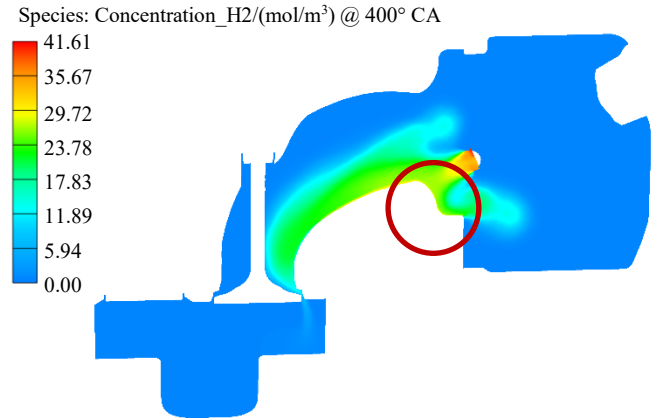


Figure 13. Visualisation of the hydrogen species concentration at 400° CA (basic variant)

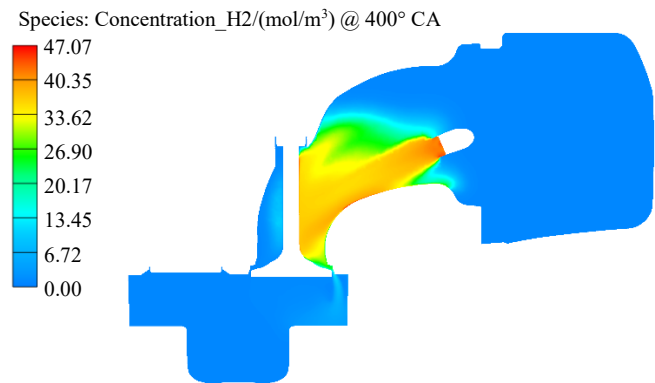


Figure 14. Visualisation of the hydrogen species concentration at 400° CA (modified variant)

Figures 15 and 16 illustrate the situation after the end of the injection process for the basic and the modified variant. It can be seen that for the basic variant, mixture accumulations remain in the manifold even after injection has ended and are not fed to the cylinder in contrast to the modified variant. This reduces the effective fuel quantity fed to the respective cylinder, which in turn leads to reduced IMEP of this cylinder and very probably also to losses in overall engine efficiency.

Due to the lateral deflection of the hydrogen flow observed with the basic variant, there is also a risk that the adjacent cylinders might be supplied with more fuel than intended, which further contributes to the unequal fuel distribution across the cylinders which has been observed experimentally. The use of the modified variant should also reduce the risk of backfire by avoiding fuel accumulation in the manifold and the intake ports after completion of gas exchange.

However, as illustrated by Figure 16, there is still potential for further optimisation with regard to mixture formation and homogenisation in the modified variant. Injection into the swirl channel, thus using the intake charge movement around the cylinder vertical axis for better mixing, might further improve fuel homogenisation inside the cylinder. This will be investigated in the future as part of further studies and experimental investigations on the engine test bench.

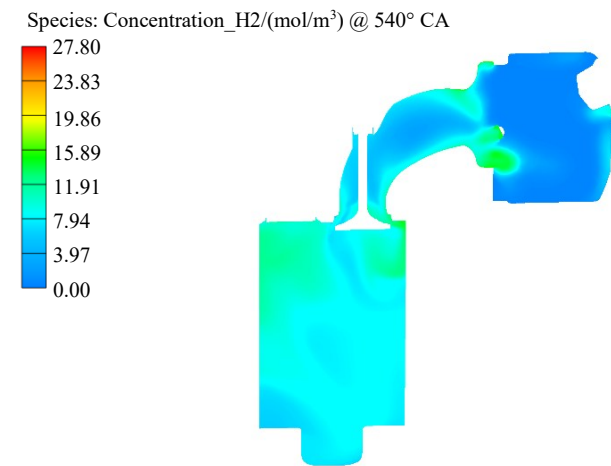


Figure 15. Visualisation of the hydrogen species concentration at 540° CA (basic variant)

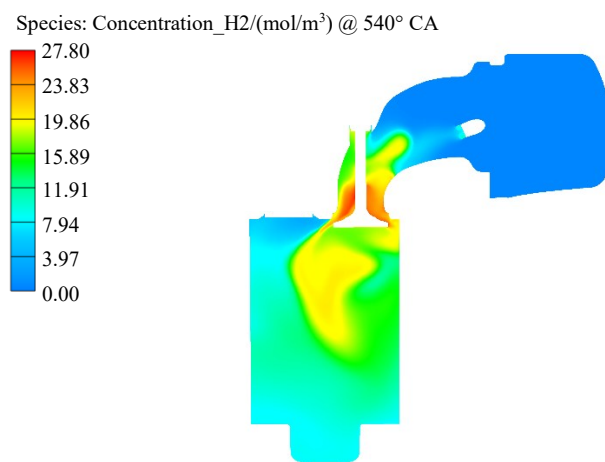


Figure 16. Visualisation of the hydrogen species concentration at 540° CA (modified variant)

Summary and Conclusions

In the work presented here, two variants of a hydrogen injection tubes were analysed in terms of fluid mechanics and compared with each other. The design of the modified variant was based on simulative analyses of the internal manifold flow of the engine previously tested experimentally on the test bench.

It was revealed that the design of the basic variant is rather unfavourable with regard to the direction of fuel injection due to the specific geometric boundary conditions leading to a deflection of the injection jet in the area of the intake port and an unwanted accumulation of a part of the fuel in the manifold. This issue could be solved with the modified variant of the injection tube, which slightly protrudes into the engine's filling port, which leads to the injection process being less dependent of the internal flow in the manifold. In subsequent investigations, the rotational alignment of the modified

variant will be further analysed in order to further reduce the uneven mixture distribution observed in the simulation.

References

1. Klell, M., Eichlseder, H., Trattner, A. (2023). Energy Revolution and Hydrogen Economy. In: Hydrogen in Automotive Engineering. Springer, Wiesbaden. https://doi.org/10.1007/978-3-658-35061-1_1
2. Kraftfahrtbundesamt [German Federal Motor Transport Authority] (2023), "Pressemitteilungen - Der Fahrzeugbestand am 1. Januar 2023." [Press releases - The vehicle fleet on January 1, 2023]. Accessed March 20, 2024. https://www.kba.de/DE/Presse/Pressemitteilungen/Fahrzeugbestand/2023/pm08_fz_bestand_pm_komplett.html
3. Klepatz, K., Konradt, S., Tempelshagen, R., Rottengruber, H. (2021). System comparison CO2-free commercial vehicle drives. In: Berns et al. (eds) Commercial Vehicle Technology 2020/2021. Proceedings. Springer Vieweg, Wiesbaden. https://doi.org/10.1007/978-3-658-29717-6_13.
4. Frey, H., Golze, K., Hirscher, M., Felderhoff, M. (2023). Chemisches Element Wasserstoff. In: Energieträger Wasserstoff. Energie in Naturwissenschaft, Technik, Wirtschaft und Gesellschaft. Springer Vieweg, Wiesbaden. https://doi.org/10.1007/978-3-658-40967-8_1
5. Pannek, C., Lambrecht, A., Wöllenstein, J., Buse, K., Keßler, A., Tschuncky, R., Jäckel, P., Quirin, S., Oeckl, S., Youssef, S., Hermann, H.-G. (2022). Sensorik und Sicherheit. In: Neugebauer, R. (eds) Wasserstofftechnologien. Springer Vieweg, Berlin, Heidelberg. https://doi.org/10.1007/978-3-662-64939-8_14
6. Rezai, R., Hayduk, C., Sens, M., Fandakov, A., Bertram, C. (2020). "Hydrogen Combustion – a Puzzle Piece of Future Sustainable Transportation!", SIA Powertrain & Energy
7. Eicheldinger S, Karmann S, Prager M, Wachtmeister G. Optical screening investigations of backfire in a large bore medium speed hydrogen engine. International Journal of Engine Research. 2022;23(5):893-906. doi:10.1177/14680874211053171

Contact Information

Philipp Jung, M.Sc.
 RPTU University of Kaiserslautern-Landau
 Institute of Vehicle Propulsion Systems (LAF)
 Gottlieb-Daimler-Str. 44
 D-67663 Kaiserslautern/Germany
 E-Mail: philipp.jung@mv.rptu.de

Acknowledgments

The work presented here was carried out within the framework of the project "WaVe", funded by the German Federal Ministry for Economic Affairs and Climate Action (BMWK) and the European Union with the TÜV Rheinland Consulting GmbH as project management organization. The authors would like to express their gratitude for this funding. Furthermore, the authors would like to thank all the project partners for their support throughout the project. Particular thanks go to FEV for their support in converting the base engine to hydrogen operation and to Daimler Truck for providing the engine and spare parts.

Definitions/Abbreviations

| | |
|--------------|---|
| CA | Crank Angle |
| CFD | Computational Fluid Dynamics |
| EGR | Exhaust Gas Recirculation |
| FC | Fuel Cell |
| ICE | Internal Combustion Engine |
| IMEP | Indicated Mean Effective Pressure |
| MFB50 | 50% Mass Fraction Burned (Centre of Combustion, $A_{i,50}$) |
| NEDC | New European Driving Cycle |
| PFI | Port Fuel Injection |
| RANS | Reynolds Averaged Navier Stokes |
| TDC | Top Dead Centre |